Acadlore Transactions on Applied Mathematics and Statistics
https://www.acadlore.com/journals/ATAMS

On Computing Degree-Based Topological Invariants for Special Graphs

Kiran Naz[1], Hafiz Muhammad Bilal[2*], Sarfraz Ahmad[1]

[1] Department of Mathematics, COMSATS University Islamabad, Lahore Campus, 54000 Lahore, Pakistan
[2] Department of Mathematics, Lahore Garrison University, 54000 Lahore, Pakistan

* Correspondence: Hafiz Muhammad Bilal (hm.bilal@lgu.edu.pk)

Received: 05-10-2025 **Revised:** 06-20-2025 **Accepted:** 06-27-2025

Citation: K. Naz, H. M. Bilal, and S. Ahmad, "On computing degree-based topological invariants for special graphs," *Acadlore Trans. Appl Math. Stat.*, vol. 3, no. 2, pp. 143–157, 2025. https://doi.org/10.56578/atams030205.

© 2025 by the author(s). Published by Acadlore Publishing Services Limited, Hong Kong. This article is available for free download and can be reused and cited, provided that the original published version is credited, under the CC BY 4.0 license.

Abstract: Topological indices represent an important class of mathematical tools for studying the structural properties of graphs and have various applications in mathematical chemistry, especially in analyzing the structural properties of molecules and quantitative structure-activity relationship. Among degree-based topological indices based on degree, the Sombor indices are useful in determining the structural properties of graphs based on the degrees of adjacent vertices. In this paper, the Sombor index (SO), the reduced Sombor index (SO_{red}), and the average Sombor index (SO_{avg}) of several special graph classes were studied. These include the Web graphs, Windmill graphs, Dutch Windmill graphs, double graphs of Dutch Windmill graphs, and strong double graphs of Dutch Windmill graphs. Degree partitions of these special graph classes were calculated and the expressions of three Sombor indices were determined using structural parameters. These expressions were then analyzed numerically and graphically in order to investigate the behavior of the Sombor type indices as the graph parameters increased. It was found numerically that all three Sombor indices exhibited an increasing trend over the range of parameters considered and consistently satisfied the order $SO(G) > SO_{\text{red}}(G) > SO_{\text{avg}}(G)$. Furthermore, the double and strong double graphs had considerably higher Sombor indices when compared to their corresponding Dutch Windmill graphs. This shows how adding more connections to a graph increases the degree-based Sombor descriptors. From the above results, one can conclude that the Sombor type indices successfully reflect the variation in the degree distribution and connectivity arising from different graph constructions.

Keywords: Sombor indices; Web graph; Windmill graph; Dutch windmill graph; Double graph of Dutch windmill graph; Strong double graph of Dutch windmill graph

1 Introduction

The origin of graph theory was traditionally dated back to year 1736, when Euler solved the famous Königsberg bridges problem [1]. Graph theory is one of the few mathematical areas of study that have an exact date of emergence. Kirchhoff's research into electrical networks directed his progress of basic theory as well as ideas about trees in graphs, while Cayley considered trees from the calculation of isomers as living chemicals. Another form of graph paradox was suggested by Hamilton. Graph theory, a branch of mathematics relating to network points connected by lines, has its origin in recreational mathematical problems but has grown into the core of mathematical research through chemistry, occupational research, social science, and computer science. A graph G consists of a set of nodes $V = \{u_1, u_2, u_3, \ldots\}$ and the other set $E = \{e_{i_1}, e_{i_2}, e_{i_3}, \ldots\}$ whose elements are called arcs. If $e_i = u_1u_2$ is an arc of graph G, then the nodes u_1 and u_2 are adjacent in G. When any two nodes are connected by more than one arc, the graph is called a multigraph. A numerical value associated with each node is its degree.

The topological descriptor is the nominal value associated with the graph and must be a structural variable. Several topological descriptors have been described and most of them have found properties as a modeling of chemicals, drugs, and other molecular structures. The Wiener index [2–4] is the first topological descriptor used in chemistry. Topological descriptors are statistical measures of a graph of cells that remain constant under the graph isomorphism. Started their journey in 1947, a wide variety of topological descriptors have been created and much work has been done on graphs of various cells and networks. Likewise, Harold Wiener introduced and developed this intriguing guide to determine the physical characteristics of alkane species known as paraffin in 1947. Topological descriptors are of incompatible types as degree-based topological descriptors, distance-based topological descriptors,

and spectrum-based [5, 6] topological descriptors. To adopt an applied mathematical approach, graphs like web, windmill, and Dutch windmill graphs are very useful and idealized models of networks having a central or a well-connected center along with peripheral or repeating components. These graphs can be used to model connectivity patterns in case of molecular and chemical networks, communication or transport networks, and many other types of complex network models that include interaction between a few well-connected units and many other less connected units. In the case of the chemical graph model, such a type of family of graphs is quite suitable to depict simple models of molecular frameworks involving branchings and repeating parts of molecules along with the concept of hubs. The use of double and strong double construction allows us to investigate the effect of increasing connectivity and coupling between the parts of graphs [7, 8]. In this paper, the Sombor indices calculated for these graph models considered the degree of vertices as a measure of structural irregularity, and thus the comparison of these indices could be helpful in distinguishing the features of these families of graphs. This paper discussed simple graphs, which are graphs with no multiple loops and arcs. There are some important degree-based topological descriptors defined [4, 5]. The first and second Zagreb descriptors [9] are:

$$\begin{aligned} M_1(G) &= \sum_{u\in V(G)} [d_G(u)]^2 = \sum_{u_1u_2\in E(G)} [d_G(u_1) + d_G(u_2)], \\ M_2(G) &= \sum_{u_1u_2\in E(G)} [d_G(u_1) \times d_G(u_2)] \end{aligned} \tag{1}$$

In this paper $d_G(u_1)$ and $d_G(u_2)$ represent the degree of the vertices u_1 and u_2 respectively.
Suppose G show a molecular structure, then the first general Zagreb descriptor [10] was defined as:

$$M^{\beta}(G) = \sum_{u_1u_2\in E(G)} \left[d_G^{\beta-1}(u_1) + d_G^{\beta-1}(u_2)\right] \tag{2}$$

where, $\beta \neq 0$, $\beta \neq 1$ and $\beta \in \mathbb{R}$. The first degree-based invariant was defined as:

$$R(G) = \sum_{u_1\sim u_2} \frac{1}{\sqrt{d_G(u_1)\, d_G(u_2)}} \tag{3}$$

Fajtlowicz explained the Harmonic indicator in 1988 [11] and it was defined as:

$$H(G) = \sum_{u_1u_2\in E(G)} \frac{2}{d_G(u_1) + d_G(u_2)} \tag{4}$$

The inverse sum indicator [12] is stated as:

$$I(G) = \sum_{u_1,u_2\in E(G)} \frac{d_G(u_1)\, d_G(u_2)}{d_G(u_1) + d_G(u_2)} \tag{5}$$

Symmetric division indicator [13] is defined as:

$$SSD(G) = \sum_{u_1,u_2\in E(G)} \frac{\min(d_G(u_1), d_G(u_2))}{\max(d_G(u_1), d_G(u_2))} + \frac{\max(d_G(u_1), d_G(u_2))}{\min(d_G(u_1), d_G(u_2))} \tag{6}$$

The geometric arithmetic indicator was suggested by Vukičević and Furtula [14].

$$GA(G) = \sum_{u_1\sim u_2} \frac{\sqrt{d_G}(u_1)\, d_G(u_2)}{\frac{1}{2}[d_G(u_1) + d_G(u_2)]} \tag{7}$$

In the following section, the degree-based Sombor descriptors are calculated. These Sombor descriptors [15–19] are defined as:

$$\begin{aligned} SO(G) &= \sum_{u_1u_2\in E(G)} \sqrt{d_G(u_1)^2 + d_G(u_2)^2}, \\ SO_{\text{red}}(G) &= \sum_{u_1u_2\in E(G)} \sqrt{(d_G(u_1) - 1)^2 + (d_G(u_2) - 1)^2}, \\ SO_{\text{avg}}(G) &= \sum_{u_1u_2\in E(G)} \sqrt{\left(d_G(u_1) - \frac{2m}{n}\right)^2 + \left(d_G(u_2) - \frac{2m}{n}\right)^2} \end{aligned} \tag{8}$$

We discussed web, windmill, Dutch windmill, double graph, and strong double graph of Dutch windmill [20–22] with the assistance of Sombor index. The chemical property of the Sombor indicator, mainly the capability to discriminate and speculate, was explored by Gutman et al. [23] and Shigehalli and Chougale [24]; obviously the Sombor index has gained considerable awareness in chemistry and mathematics. In this research work, the Sombor indices of five particular families of graphs have been studied, starting from the process of formation of the graph family to degree study, mathematical calculation, numerical computation, and comparison. In the current scenario p, represents the size or order of the complete graph component (the number of vertices in each complete subgraph), and r is the number of complete graph components used in the formation of the graph family. There are three Sombor-type parameters considered in the current study: Sombor index SO, reduced Sombor index SO_{red}, and average Sombor index SO_{avg}. It has been found that SO takes the maximum values while SO_{avg} takes the minimum values. The complete methodology of this study is illustrated in Figure 1 below.

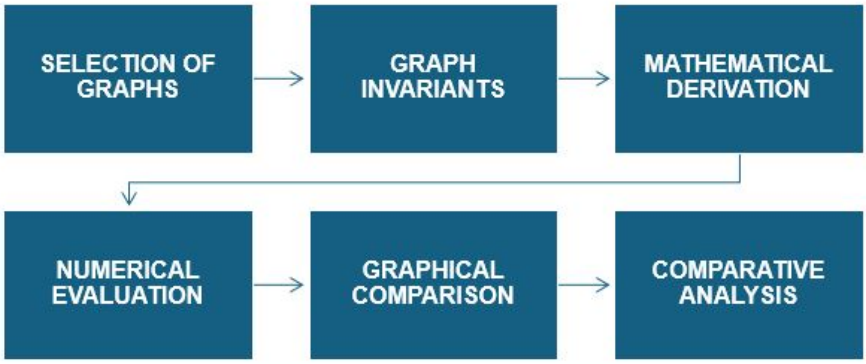


Figure 1. A flowchart showing the workflow of the methodology

2 Major Results of Sombor Indices for the Special Graphs

2.1 Web Graph

The web graph $W_{p,r}$ was obtained by taking r copies of the cycle graph C_p as described in Figure 2. A web graph has been defined equivalently as a prism graph. The order of the web graph is pr and size $p(2r-1)$. In the web graph, we have the following sets of edge partition:

$$E_1 = \left\{u_iu_j \in E(W_{p,r}) \mid d_{W_{p,r}}(u_i) = d_{W_{p,r}}(u_j) = 3\right\},$$
$$E_2 = \left\{u_iu_j \in E(W_{p,r}) \mid d_{W_{p,r}}(u_i) = 3,\ d_{W_{p,r}}(u_j) = 4\right\},$$
$$E_3 = \left\{u_iu_j \in E(W_{p,r}) \mid d_{W_{p,r}}(u_i) = d_{W_{p,r}}(u_j) = 4\right\}$$

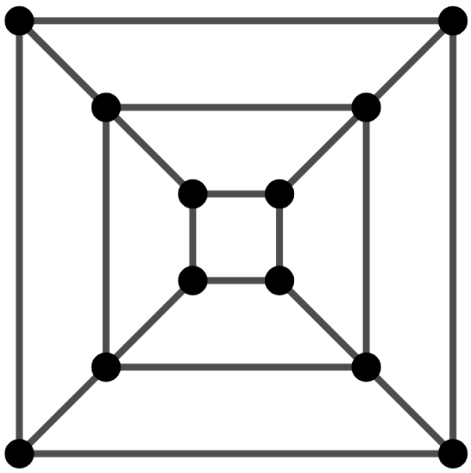


Figure 2. Web graph $W_{3,3}$

For $p = 4$ and $r = 3$, we computed non-identical Sombor indices of $W_{4,3}$:

$$SO\left[W_{4,3}\right] = 40 + 40\sqrt{2},$$
$$SO_{red}\left[W_{4,3}\right] = 8\sqrt{13} + 28\sqrt{2},$$
$$SO_{avg}\left[W_{4,3}\right] = \frac{8\sqrt{65} + 60\sqrt{2}}{3}$$

The final description of the web graph for non-identical Sombor descriptors are given in theorem (1), (2), and (3).

Theorem 1. Suppose $W_{p,r}$ represent a web graph and $O|W_{p,r}| = pr$. Then, the SO of $W_{p,r}$ is

$$SO\left(W_{p,r}\right) = 2p\sqrt{18} + 10p + p(2r-5)\sqrt{32} \tag{9}$$

Proof. For $p \geq 3$ and $r \geq 3$, consider $W_{p,r}$ as a web graph with $O|W_{p,r}| = pr$. We know,

$$SO\left(W_{p,r}\right) = \sum_{u_iu_j \in E(W_{p,r})} \sqrt{d_G(u_i)^2 + d_G(u_j)^2},$$
$$SO\left(W_{p,r}\right) = 2p\sqrt{18} + 10p + p(2r-5)\sqrt{32}$$

Theorem 2. Let $W_{p,r}$ represent a web graph and $O|W_{p,r}| = pr$. Then, the SO_{red} of $W_{p,r}$ is

$$SO_{\text{red}}\left(W_{p,r}\right) = 2p\sqrt{8} + 2p\sqrt{13} + p(2r-5)\sqrt{18} \tag{10}$$

Proof. For $p \geq 3$ and $r \geq 3$, consider $W_{p,r}$ as a web graph with $O|W_{p,r}| = pr$. We know,

$$SO_{\text{red}}\left(W_{p,r}\right) = \sum_{u_iu_j \in E(W_{p,r})} \sqrt{\left(d_G(u_i) - 1\right)^2 + \left(d_G(u_j) - 1\right)^2},$$
$$SO_{\text{red}}\left(W_{p,r}\right) = 2p\sqrt{8} + 2p\sqrt{13} + p(2r-5)\sqrt{18}$$

Theorem 3. Suppose $W_{p,r}$ represent a web graph and $O|W_{p,r}| = pr$. Then, the SO_{avg} of $W_{p,r}$ is

$$\begin{aligned} SO_{\text{avg}}\left(W_{p,r}\right) = p\sqrt{2}\sqrt{\left(3 - \frac{p(2r-1)}{pr}\right)^2} + 2p\sqrt{\left(3 - \frac{p(2r-1)}{pr}\right)^2 + \left(4 - \frac{p(2r-1)}{pr}\right)^2} \\ + p(2r-5)\sqrt{2}\sqrt{\left(4 - \frac{p(2r-1)}{pr}\right)^2} \end{aligned} \tag{11}$$

Proof. For $p \geq 3$ and $r \geq 3$, consider $W_{p,r}$ as a web graph with $O|W_{p,r}| = pr$. We know,

$$SO_{\text{avg}}\left(W_{p,r}\right) = \sum_{u_iu_j \in E(W_{p,r})} \sqrt{\left(d_G(u_i) - \frac{2m}{n}\right)^2 + \left(d_G(u_j) - \frac{2m}{n}\right)^2}$$

Therefore, it necessitates the outcome.

After having outcomes from theorem (1), (2), and (3), we computed the relationship [18] among the results of SO, SO_{red}, and SO_{avg} of a web graph. Figure 3 and Table 1 define the graphic and numeric forms of these descriptors.

Table 1 reveals the consistent increase of the three Sombor indices. For every value considered, the indices satisfy:

$$SO(W_{p,r}) > SO_{\text{red}}(W_{p,r}) > SO_{\text{avg}}(W_{p,r})$$

The growth is substantial: from $(p, r) = (3, 3)$ to $(10, 10)$, SO, SO_{red}, and SO_{avg} increased by factors of approximately 14.27, 14.90, and 16.05, respectively. Moreover, at $(10, 10)$, $SO_{\text{red}}/SO \approx 0.740$ and $SO_{\text{avg}}/SO \approx 0.492$. Thus, although all three indices exhibit similar increasing behavior, SO_{avg} shows the comparatively stronger relative growth over this range.

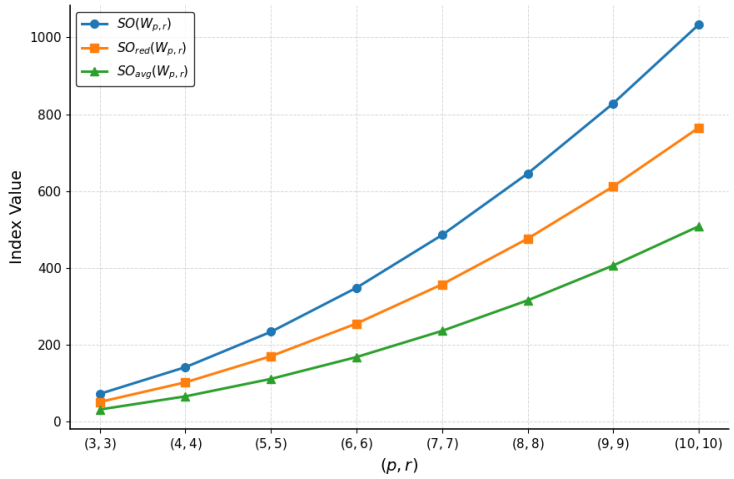


Figure 3. Comparison of Sombor indices of the web graph

Note: SO = Sombor index; SO_{red} = reduced Sombor index; SO_{avg} = average Sombor index. $(W_{p,r})$ represents Sombor indices of the web graph.

Table 1. Comparison of SO, SO_{red}, and SO_{avg} for web graph

(p, r)	$SO(W_{p,r})$	$SO_{\text{red}}(W_{p,r})$	$SO_{\text{avg}}(W_{p,r})$
$(3, 3)$	72.4264	51.3318	31.6809
$(4, 4)$	141.8234	102.3835	65.8461
$(5, 5)$	233.8478	170.4058	111.3270
$(6, 6)$	348.4996	255.3986	168.1226
$(7, 7)$	485.7788	357.3621	236.2325
$(8, 8)$	645.6854	476.2960	315.6566
$(9, 9)$	828.2195	612.2006	406.3947
$(10, 10)$	1,033.3810	765.0757	508.4467

Note: p represents order of a complete graph and r represents copies of complete graphs. SO = Sombor index; SO_{red} = reduced Sombor index; SO_{avg} = average Sombor index. $(W_{p,r})$ represents Sombor indices of the web graph.

2.2 Windmill Graph

The windmill graph W_p^r was constructed by using r copies of the complete graph with a common node as shown in Figure 4. The windmill graph [23] is isomorphic to $rK_{p-1} + K_1$. The $O|W_p^r|$ is $r(p-1)+1$, and size $\frac{rp(p-1)}{2}$. In the windmill graph, we have the following sets of edge partition:

$$E_1 = \left\{u_iu_j \in E(W_p^r) \mid d_{W_p^r}(u_i) = d_{W_p^r}(u_j) = p-1\right\},$$
$$E_2 = \left\{u_iu_j \in E(W_p^r) \mid d_{W_p^r}(u_i) = p-1,\ d_{W_p^r}(u_j) = r(p-1)\right\}$$

For $p = 3$ and $r = 3$, we computed non-identical Sombor indices of $[W_3^3]$:

$$SO[W_3^3] = 12\sqrt{10} + 6\sqrt{2},$$
$$SO_{\text{red}}[W_3^3] = 6\sqrt{26} + 3\sqrt{2},$$
$$SO_{\text{avg}}[W_3^3] = \frac{24\sqrt{37}}{7} + \frac{12\sqrt{2}}{7}$$

The final description of the windmill graph for non-identical Sombor descriptors were given in theorem (4), (5), and (6).

Theorem 4. Let W_p^r represent a windmill graph and $O|W_p^r| = 2p-1$. Then, the SO of W_p^r is

$$SO(W_p^r) = r(p-1)\sqrt{(p-1)^2 + (r(p-1))^2} + \frac{r\sqrt{2}}{2}(p-1)^2(p-2) \tag{12}$$

Proof. By letting W_p^r as a windmill graph and $O|W_p^r| = 2p-1$, where $r \geq 2$ and $p \geq 3$. We know,

$$SO(W_p^r) = \sum_{u_iu_j \in E(W_p^r)} \sqrt{d_G(u_i)^2 + d_G(u_j)^2},$$

$$SO(W_p^r) = r(p-1)\sqrt{(p-1)^2 + (r(p-1))^2} + \frac{r\sqrt{2}}{2}(p-1)^2(p-2)$$

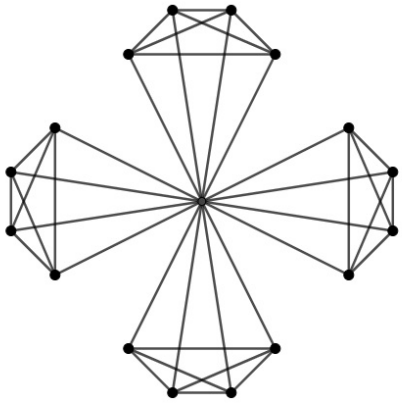


Figure 4. Windmill graph W_5^4

Theorem 5. Suppose W_p^r is a windmill graph with $O|W_p^r| = 2p-1$. Then,

$$SO_{\text{red}}(W_p^r) = r(p-1)\sqrt{(p-2)^2 + ((r-1)(p-1)+(p-2))^2} + \frac{r}{2}\sqrt{2}(p-1)(p-2)^2 \tag{13}$$

Proof. By letting W_p^r as a windmill graph and $O|W_p^r| = 2p-1$, where $r \geq 2$ and $p \geq 3$. We know,

$$SO_{\text{red}}(W_p^r) = \sum_{u_iu_j \in E(W_p^r)} \sqrt{(d_G(u_i)-1)^2 + (d_G(u_j)-1)^2},$$

$$SO_{\text{red}}(W_p^r) = r(p-1)\sqrt{(p-2)^2 + ((p-1)(p-1)+(p-2))^2} + \frac{r}{2}\sqrt{2}(p-1)(p-2)^2.$$

Theorem 6. Let W_p^r be a windmill graph and $O|W_p^r| = 2p-1$. Then, the SO_{avg} of W_p^r is

$$\begin{aligned} SO_{\text{avg}}(W_p^r) = r(p-1)\sqrt{\left((p-1) - \left(\frac{pr(p-1)}{r(p-1)+1}\right)\right)^2 + \left(r(p-1) - \left(\frac{rp(p-1)}{r(p-1)+1}\right)\right)^2} \\ + \frac{r\sqrt{2}}{2}(p-1)(p-2)\sqrt{\left((p-1) - \frac{rp(p-1)}{r(p-1)+1}\right)^2} \end{aligned} \tag{14}$$

Proof. By letting W_p^r as a windmill graph and $O|W_p^r| = 2p-1$, where $r \geq 2$ and $p \geq 3$. We know,

$$SO_{\text{avg}}(W_p^r) = \sum_{u_iu_j \in E(W_p^r)} \sqrt{\left(d_G(u_i) - \frac{2m}{n}\right)^2 + \left(d_G(u_j) - \frac{2m}{n}\right)^2}$$

Therefore, it necessitates the outcome.

After getting values from theorem (4), (5), and (6), we computed the relationship [18] between the results of Sombor descriptors of a windmill graph. The graphical and numerical comparison of these descriptors are available in Figure 5 and Table 2.

Table 2 indicates a pronounced increase in all three Sombor indices. The ordering remains unchanged throughout the table:

$$SO(W_p^r) > SO_{\text{red}}(W_p^r) > SO_{\text{avg}}(W_p^r)$$

The increase is considerably faster than that observed for the web graph. From $(p, r) = (3, 3)$ to $(10, 10)$, SO, SO_{red}, and SO_{avg} increased by factors of approximately 274.00, 347.77, and 329.19, respectively. At $(10, 10)$, the ratios SO_{red}/SO and SO_{avg}/SO were approximately 0.952 and 0.602, respectively. These results demonstrated the rapid growth of the indices for the windmill graph as both parameters increased.

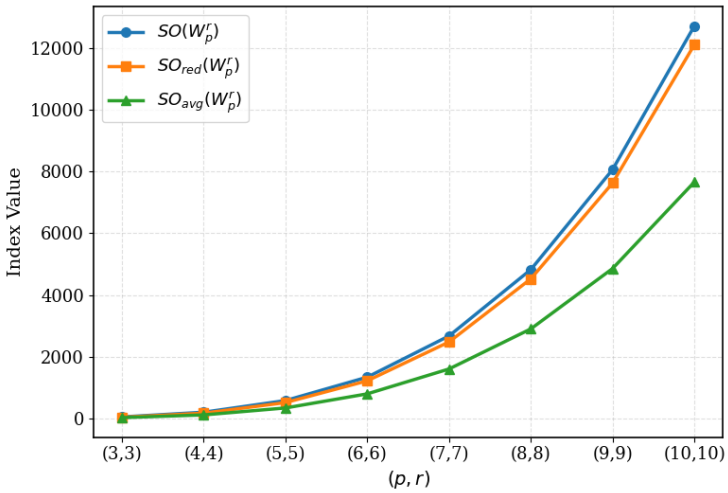


Figure 5. Comparison of Sombor indices of the windmill graph

Note: SO = Sombor index; SO_{red} = reduced Sombor index; SO_{avg} = average Sombor index. (W_p^r) represents Sombor indices of the Windmill graph.

Table 2. Comparison of SO, SO_{red}, and SO_{avg} for windmill graph

(p, r)	$SO(W_p^r)$	$SO_{\text{red}}(W_p^r)$	$SO_{\text{avg}}(W_p^r)$
$(3, 3)$	46.4326	34.8367	23.2796
$(4, 4)$	199.3435	168.1052	111.7867
$(5, 5)$	577.6272	511.9869	337.4675
$(6, 6)$	1,336.6784	1,217.6481	794.6393
$(7, 7)$	2,672.8636	2,477.2197	1,601.5750
$(8, 8)$	4,823.5202	4,523.8003	2,900.5317
$(9, 9)$	8,066.9564	7,631.4577	4,857.7594
$(10, 10)$	12,722.4512	12,115.2295	7,663.5051

Note: p represents order of a complete graph and r represents copies of complete graphs. SO = Sombor index; SO_{red} = reduced Sombor index; SO_{avg} = average Sombor index. (W_p^r) represents Sombor indices of the Windmill graph.

2.3 Dutch Windmill Graph

Dutch windmill graph was constructed by taking r copies of the C_p where, $p \geq 3$ joined by one common node as demonstrated in Figure 6. It was symbolized by D_p^r, where $p \geq 3$ and $r \geq 2$. The size of the Dutch windmill graph [23] is pr and $O|D_p^r| = r(p-1)+1$. In the Dutch windmill graph, we have the following sets of edge partition:

$$E_1 = \left\{ u_i u_j \in E(D_p^r) \mid d_{D_p^r}(u_i) = d_{D_p^r}(u_j) = p-1 \right\},$$

$$E_2 = \left\{ u_i u_j \in E(D_p^r) \mid d_{D_p^r}(u_i) = p-1,\ d_{D_p^r}(u_j) = 2r \right\}$$

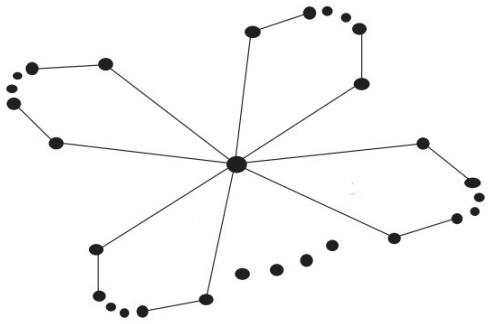


Figure 6. Dutch windmill graph

For $p = 3$ and $r = 2$, we computed non-identical Sombor indices of $[D_3^2]$:

$$SO[(D_3^2)] = 8\sqrt{5} + 4\sqrt{2},$$
$$SO_{\text{red}}[(D_3^2)] = 4\sqrt{10} + 2\sqrt{2},$$
$$SO_{\text{avg}}[(D_3^2)] = \frac{8\sqrt{17}}{5} + \frac{4\sqrt{2}}{5}$$

The final description of the Dutch windmill graph for Sombor descriptors is available in theorem (7), (8), and (9).

Theorem 7. Let D_p^r be a Dutch windmill graph and $O|D_p^r| = r(p-1)+1$. Then, the SO of D_p^r is

$$SO(D_p^r) = r(p-2)\sqrt{8} + 2r\sqrt{2^2 + (2r)^2} \tag{15}$$

Proof. By letting D_p^r as a Dutch windmill graph and $O|D_p^r| = r(p-1)+1$, where $p \geq 3$ and $r \geq 2$. We know,

$$SO(D_p^r) = \sum_{u_iu_j \in E(D_p^r)} \sqrt{d_G(u_i)^2 + d_G(u_j)^2},$$
$$SO(D_p^r) = r(p-2)\sqrt{8} + 2r\sqrt{2^2 + (2r)^2}$$

Theorem 8. Suppose D_p^r is a Dutch windmill graph and $O|D_p^r| = r(p-1)+1$. Then, the SO_{red} of D_p^r is

$$SO_{\text{red}}(D_p^r) = r(p-2)\sqrt{2} + 2r\sqrt{1 + (2r-1)^2} \tag{16}$$

Proof. By letting D_p^r be a Dutch windmill graph and $O|D_p^r| = r(p-1)+1$, where $p \geq 3$ and $r \geq 2$. We know,

$$SO_{\text{red}}(D_p^r) = \sum_{u_iu_j \in E(D_p^r)} \sqrt{(d_G(u_i)-1)^2 + (d_G(u_j)-1)^2},$$
$$SO_{\text{red}}(D_p^r) = r(p-2)\sqrt{2} + 2r\sqrt{1 + (2r-1)^2}$$

Theorem 9. Suppose D_p^r is a Dutch windmill graph and $O|D_p^r| = r(p-1)+1$. Then, the SO_{avg} of D_p^r is

$$\begin{aligned} SO_{\text{avg}}(D_p^r) &= r(p-2)\sqrt{2\left(2 - \frac{2pr}{r(p-1)+1}\right)^2} \\ &+2r\sqrt{\left(2 - \frac{2pr}{r(p-1)+1}\right)^2 + \left(2r - \frac{2pr}{r(p-1)+1}\right)} \end{aligned} \tag{17}$$

Proof. By letting D_p^r be a Dutch windmill graph and $O|D_p^r| = r(p-1)+1$, where $p \geq 3$ and $r \geq 2$. We know,

$$SO_{\text{avg}}(D_p^r) = \sum_{u_iu_j \in E(D_p^r)} \sqrt{\left(d_G(u_i) - \frac{2m}{n}\right)^2 + \left(d_G(u_j) - \frac{2m}{n}\right)^2}$$

$$SO_{\text{avg}}(D_p^r) = r(p-2)\sqrt{2}\left(2 - \frac{2pr}{r(p-1)+1}\right) + 2r\sqrt{\left(2 - \frac{2pr}{r(p-1)+1}\right)^2 + \left(2r - \frac{2pr}{r(p-1)+1}\right)}$$

By collecting results from theorem (7), (8), and (9), we computed the relationship [18] between the results of Sombor descriptors of a Dutch Windmill graph. The graphic and numeric form of these descriptors are defined in Table 3 and Figure 7.

Table 3 demonstrates that all three indices increased monotonically as $(p = r)$ from 3 to 10, while maintaining the ordering

$$SO(D_p^r) > SO_{\text{red}}(D_p^r) > SO_{\text{avg}}(D_p^r)$$

However, the relative separation between the indices was more noticeable for SO_{avg}. From $(p, r) = (3, 3)$ to $(10, 10)$, SO, SO_{red}, and SO_{avg} increased by factors of approximately 13.53, 14.17, and 7.6, respectively. At $(10, 10)$, $SO_{\text{red}}/SO \approx 0.786$, whereas $SO_{\text{avg}}/SO \approx 0.170$. Hence, SO_{avg} remains substantially smaller than the other two indices for the D_p^r.

Table 3. Comparison of SO, SO_{red}, and SO_{avg} for Dutch windmill graph

(p, r)	$SO(D_p^r)$	$SO_{\text{red}}(D_p^r)$	$SO_{\text{avg}}(D_p^r)$
$(3, 3)$	46.4326	34.8368	14.0512
$(4, 4)$	88.5971	67.8822	24.4075
$(5, 5)$	144.4068	111.7670	35.9455
$(6, 6)$	213.8686	166.4854	48.9792
$(7, 7)$	296.9848	232.0351	61.9024
$(8, 8)$	393.7567	308.4149	76.1419
$(9, 9)$	504.1848	395.6244	91.1417
$(10, 10)$	628.2692	493.6630	106.8567

Note: p represents order of a complete graph and r represents copies of complete graphs. SO = Sombor index; SO_{red} = reduced Sombor index; SO_{avg} = average Sombor index. (D_p^r) represents Sombor indices of the Dutch Windmill graph.

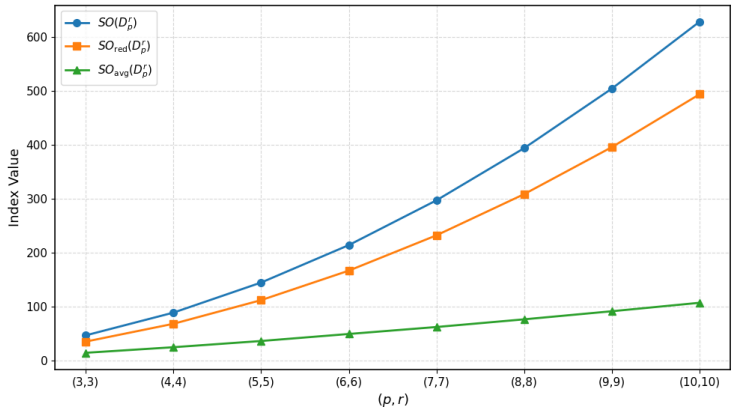


Figure 7. Comparison of Sombor indices for the Dutch windmill graph

Note: SO = Sombor index; SO_{red} = reduced Sombor index; SO_{avg} = average Sombor index. (D_p^r) represents Sombor indices of the Dutch Windmill graph.

2.4 Double Graph of Dutch Windmill Graph

The double graph of D_p^r (G) was represented by $D[G]$. In this case, two copies of G would be taken and the nodes of one copy would be connected to their respective neighbors in another copy in order to make the double graph of Dutch windmill as described in Figure 8. The order of double graph of Dutch windmill graph [23] was $2r(p-1)+2$ and size $r(5p-3)$. It was represented by $D[D_p^r]$. In double graph of Dutch windmill graph, we have the following sets of edge partition:

$$E_1 = \left\{u_iu_j \in E(D(D_p^r)) \mid d_{D(D_p^r)}(u_i) = d_{D(D_p^r)}(u_j) = 4\right\},$$
$$E_2 = \left\{u_iu_j \in E(D(D_p^r)) \mid d_{D(D_p^r)}(u_i) = 4,\ d_{D(D_p^r)}(u_j) = 3p+r\right\}$$

For $p = 3$ and $r = 2$, we computed non-identical Sombor indices of $D[D_3^2]$:

$$SO[D(D_3^2)] = 64\sqrt{5} + 32\sqrt{2},$$
$$SO_{\text{red}}[D(D_3^2)] = 16\sqrt{58} + 24\sqrt{2},$$
$$SO_{\text{avg}}[D(D_3^2)] = -\frac{32}{5} + \frac{64\sqrt{17}}{5}$$

The final description of $D(D_p^r)$ for Sombor indices were available in theorem (10), (11) and (12).

Theorem 10. Consider a graph $D(D_p^r)$ and $O|D(D_p^r)| = 2r(p-1)+2$. Then, the SO of $D(D_p^r)$ is

$$SO(D(D_p^r)) = r(3p-5)\sqrt{32} + 2r(p+1)\sqrt{(r(p+1))^2 + 4^2} \tag{18}$$

Proof. By letting $D(D_p^r)$ be a double graph of Dutch windmill graph and $O|D(D_p^r)| = 2r(p-1)+2$, where

$p \geq 3$ and $r \geq 2$. We know,

$$SO(D(D_p^r)) = \sum_{u_iu_j \in E(D(D_p^r))} \sqrt{d_G(u_i)^2 + d_G(u_j)^2},$$

$$SO(D(D_p^r)) = r(3p-5)\sqrt{32} + 2r(p+1)\sqrt{(r(p+1))^2 + 4^2}$$

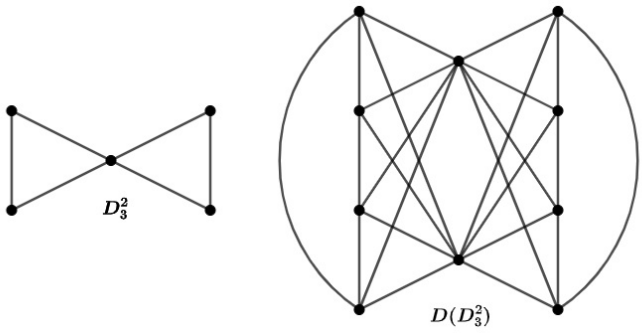


Figure 8. Double graph of Dutch windmill $D(D_p^r)$

Theorem 11. Let $D(D_p^r)$ be a double graph of Dutch windmill graph and $O|D(D_p^r)| = 2r(p-1)+2$. Then, the SO_{red} of $D(D_p^r)$ is

$$SO_{\text{red}}(D(D_p^r)) = r(3p-5)\sqrt{18} + 2r(p+1)\sqrt{(r(p+1)-1)^2 + 9} \tag{19}$$

Proof. By letting $D(D_p^r)$ be a double graph of Dutch windmill graph and $O|D(D_p^r)| = 2r(p-1)+2$, where $p \geq 3$ and $r \geq 2$. We know,

$$SO_{\text{red}}(D(D_p^r)) = \sum_{u_iu_j \in E(D(D_p^r))} \sqrt{(d_G(u_i)-1)^2 + (d_G(u_j)-1)^2},$$

$$SO_{\text{red}}(D(D_p^r)) = r(3p-5)\sqrt{18} + 2r(p+1)\sqrt{(r(p+1)-1)^2 + 9}$$

Theorem 12. Suppose $D(D_p^r)$ is a double graph of Dutch windmill graph and $O|D(D_p^r)| = 2r(p-1)+2$. Then, the SO_{avg} of $D(D_p^r)$ is

$$\begin{aligned} SO_{\text{avg}}(D(D_p^r)) &= r(3p-5)\sqrt{2\left(4 - \frac{2r(5p-3)}{2r(p-1)+2}\right)^2} \\ &+2r(p+1)\sqrt{\left(r(p+1) - \frac{2r(5p-3)}{2r(p-1)+2}\right)^2 + \left(4 - \frac{2r(5p-3)}{2r(p-1)+2}\right)^2} \end{aligned} \tag{20}$$

Proof. By letting $D(D_p^r)$ be a double graph of Dutch windmill graph, where $p \geq 3$ and $r \geq 2$. We know,

$$SO_{\text{avg}}(D(D_p^r)) = \sum_{u_iu_j \in E(D(D_p^r))} \sqrt{\left(d_G(u_i) - \frac{2m}{n}\right)^2 + \left(d_G(u_j) - \frac{2m}{n}\right)^2}$$

Therefore, it necessitates the outcome.

After obtaining general results from theorem (10), (11), and (12), we computed the relationship between the results of Sombor descriptors of a double Dutch windmill graph. The graphic and numeric comparison of indices are available in Table 4 and Figure 9.

Table 4 shows a substantial increase in all three indices as $(p = r)$ increased from 3 to 10. The ordering

$$SO(D(D_p^r)) > SO_{\text{red}}(D(D_p^r)) > SO_{\text{avg}}(D(D_p^r))$$

was preserved for all considered cases. From $(p, r) = (3, 3)$ to $(10, 10)$, the values of SO, SO_{red}, and SO_{avg} increased by factors of approximately 69.00, 77.18, and 126.06, respectively. Interestingly, the three indices became relatively closer as the graph grew; for example, at $(10, 10)$, $SO_{\text{red}}/SO \approx 0.977$ and $SO_{\text{avg}}/SO \approx 0.916$. Compared with the original Dutch windmill graph, the double construction therefore produced substantially larger index values and noticeably changed their relative growth, particularly for SO_{avg}.

Table 4. Comparison among SO, SO_{red}, and SO_{avg} for double graph of Dutch windmill graph

(p, r)	$SO(D(D_p^r))$	$SO_{\text{red}}(D(D_p^r))$	$SO_{\text{avg}}(D(D_p^r))$
$(3, 3)$	371.4609	324.5538	186.2364
$(4, 4)$	974.2350	888.2093	641.5529
$(5, 5)$	2,098.7722	1,961.4176	1,575.1168
$(6, 6)$	3,985.1985	3,784.1332	3,225.9649
$(7, 7)$	6,921.5473	6,644.3326	5,881.7140
$(8, 8)$	11,243.8295	10,878.0041	9,878.1883
$(9, 9)$	17,336.0492	16,869.1414	15,599.2976
$(10, 10)$	25,630.2083	25,049.7410	23,476.9913

Note: p represents order of a complete graph and r represents copies of complete graphs. SO = Sombor index; SO_{red} = reduced Sombor index; SO_{avg} = average Sombor index. $(D(D_p^r))$ represents Sombor indices of the double graph of Dutch windmill graph.

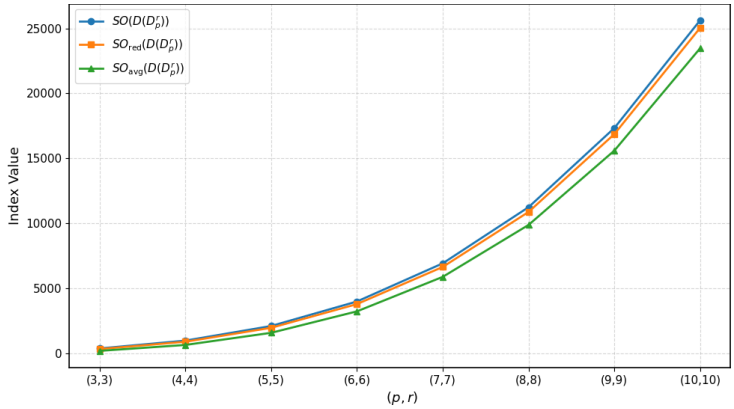


Figure 9. Comparison of Sombor indices for the double graph of Dutch windmill graph

Note: SO = Sombor index; SO_{red} = reduced Sombor index; SO_{avg} = average Sombor index. $(D(D_p^r))$ represents Sombor indices of the double graph of Dutch windmill graph.

2.5 Double Graph of Strong Dutch Windmill Graph

The strong $D[G]$ was derived from considering both graphs such that the closed adjacent of each vertex in one graph was paired with the adjacent vertex in another graph. The strong double graph [23] of a Dutch windmill graph is represented by $SD[D_p^r]$ as shown in Figure 10. The order of a $SD(D_p^r)$ was $2r(p-1)+2$ and size $r(p-1)(p+2)+(r(p+1)+1)$. In strong double graph of Dutch windmill graph, we have the following sets of edge partition:

$$E_1 = \left\{u_iu_j \in E(SD(D_p^r)) \mid d_{SD(D_p^r)}(u_i) = d_{SD(D_p^r)}(u_j) = p+2\right\},$$
$$E_2 = \left\{u_iu_j \in E(SD(D_p^r)) \mid d_{SD(D_p^r)}(u_i) = p+2,\ d_{SD(D_p^r)}(u_j) = 4p+r+1\right\}$$

For $p = 3$ and $r = 2$, we computed three different Sombor descriptors of $SD[D_3^2]$:

$$SO[SD(D_3^2)] = 12\sqrt{2} + 9\sqrt{212}$$
$$SO_{\text{red}}[SD(D_3^2)] = 12\sqrt{2} + 32\sqrt{10}$$
$$SO_{\text{avg}}[SD(D_3^2)] = 13\sqrt{2} + \frac{142}{9}$$

The final representation of the $SD(D_p^r)$ for non-identical Sombor indices are available in theorem (13), (14), and (15).

Theorem 13. Consider a graph $SD(D_p^r)$ and $O|SD(D_p^r)| = 2r(p-1)+2$. Then, the SO of $SD(D_p^r)$ is

$$SO(SD(D_p^r)) = r(p^2-3)\sqrt{2(p+2)^2} + \sqrt{2(r(p+1)+1)^2} + 2r(p+1)\sqrt{(r(p+1)+1)^2 + (p+2)^2} \tag{21}$$

Proof. By letting $SD(D_p^r)$ be a strong $D(D_p^r)$ and $O|SD(D_p^r)| = 2r(p-1)+2$, where $p \geq 3$ and $r \geq 2$. We know,

$$SO(SD(D_p^r)) = \sum_{u_iu_j \in E(SD(D_p^r))} \sqrt{d_G(u_i)^2 + d_G(u_j)^2},$$

$$SO(SD(D_p^r)) = r(p^2-3)\sqrt{2(p+2)^2} + \sqrt{2(r(p+1)+1)^2} + 2r(p+1)\sqrt{(r(p+1)+1)^2 + (p+2)^2}$$

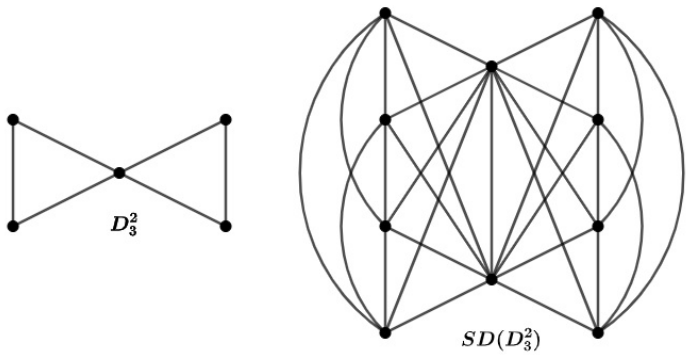


Figure 10. Strong double graph of Dutch windmill graph

Theorem 14. Consider a graph $SD(D_p^r)$ and $O|SD(D_p^r)| = 2r(p-1)+2$. Then, the SO_{red} of $SD(D_p^r)$ is

$$SO_{\text{red}}(SD(D_p^r)) = r(p^2-3)\sqrt{2(p+1)^2} + \sqrt{2(r(p+1))^2} + 2r(p+1)\sqrt{(r(p+1))^2 + (p+1)^2} \tag{22}$$

Proof. By letting $SD(D_p^r)$ be a strong $D(D_p^r)$ and $O|SD(D_p^r)| = 2r(p-1)+2$, where $p \geq 3$ and $r \geq 2$. We know,

$$SO_{\text{red}}(SD(D_p^r)) = \sum_{u_iu_j \in E(SD(D_p^r))} \sqrt{(d_G(u_i)-1)^2 + (d_G(u_j)-1)^2},$$

$$SO_{\text{red}}(SD(D_p^r)) = r(p^2-3)\sqrt{2(p+1)^2} + \sqrt{2(r(p+1))^2} + 2r(p+1)\sqrt{(r(p+1))^2 + (p+1)^2}.$$

Theorem 15. Consider a graph $SD(D_p^r)$ and $O|SD(D_p^r)| = 2r(p-1)+2$. Then, the SO_{avg} of $SD(D_p^r)$ is

$$\begin{aligned} SO_{\text{avg}}(SD(D_p^r)) = 2r(p+1)&\sqrt{\left((r(p+1)+1) - \frac{2m}{2r(p-1)+2}\right)^2 + \left((p+2) - \frac{2m}{2r(p-1)+2}\right)^2} \\ &+ r(p^2-3)\sqrt{2\left((p+2) - \frac{2m}{2r(p-1)+2}\right)^2} \\ &+ \sqrt{2\left((r(p+1)+1) - \frac{2m}{2r(p-1)+2}\right)^2} \end{aligned} \tag{23}$$

where, $2m = 2r(p-1)(p+2) + 2(r(p+1)+1)$.

Proof. By letting $SD(D_p^r)$ be a strong $D(D_p^r)$ and $O|SD(D_p^r)| = 2r(p-1)+2$, where $p \geq 3$ and $r \geq 2$. We know,

$$SO_{\text{avg}}(SD(D_p^r)) = \sum_{u_iu_j \in E(SD(D_p^r))} \sqrt{\left(d_G(u_i) - \frac{2m}{n}\right)^2 + \left(d_G(u_j) - \frac{2m}{n}\right)^2}$$

Hence, it follows the result.

By obtaining results from theorem (13), (14), and (15), we computed the relationship between the results of Sombor descriptors of a $SD(D_p^r)$. The graphic and numeric comparison of descriptors are provided in Table 5 and Figure 11.

Table 5 confirms a consistently increasing trend for all three Sombor indices as $(p = r)$ increased from 3 to 10, with

$$SO(SD(D_p^r)) > SO_{\text{red}}(SD(D_p^r)) > SO_{\text{avg}}(SD(D_p^r))$$

throughout the considered range. From $(p, r) = (3, 3)$ to $(10, 10)$, SO, SO_{red}, and SO_{avg} increased by factors of approximately 85.80, 93.68, and 112.69, respectively. At $(10, 10)$, the ratios calculated were $SO_{\text{red}}/SO \approx 0.961$ and $SO_{\text{avg}}/SO \approx 0.563$. The strong double construction therefore produced a further substantial increase in the magnitude of the indices. For example, at $(10, 10)$, the SO and SO_{red} values of the strong double graph were approximately 65.55 and 80.15 times, respectively; for those of the corresponding Dutch windmill graph, SO_{avg} was approximately 216.86 times larger. This indicates that the additional connectivity introduced by the strong double construction has a pronounced effect on the growth of the Sombor indices.

Table 5. Comparison of SO, SO_{red}, and SO_{avg} for strong double graph of Dutch windmill graph

(p, r)	$SO(SD(D_p^r))$	$SO_{\text{red}}(SD(D_p^r))$	$SO_{\text{avg}}(SD(D_p^r))$
$(3, 3)$	479.9453	422.3726	205.6313
$(4, 4)$	1,344.5463	1,220.6009	660.2001
$(5, 5)$	3,039.6149	2,811.4544	1,583.2535
$(6, 6)$	5,974.9053	5,596.1613	3,210.7874
$(7, 7)$	10,642.0901	10,057.8868	5,827.0961
$(8, 8)$	17,614.7715	16,761.7354	9,764.5776
$(9, 9)$	27,548.4869	26,354.7517	15,403.6726
$(10, 10)$	41,180.7117	39,565.9212	23,172.8414

Note: p represents order of a complete graph and r represents copies of complete graphs. SO = Sombor index; SO_{red} = reduced Sombor index; SO_{avg} = average Sombor index. $(SD(D_p^r))$ represents Sombor indices of the strong double graph of Dutch windmill graph.

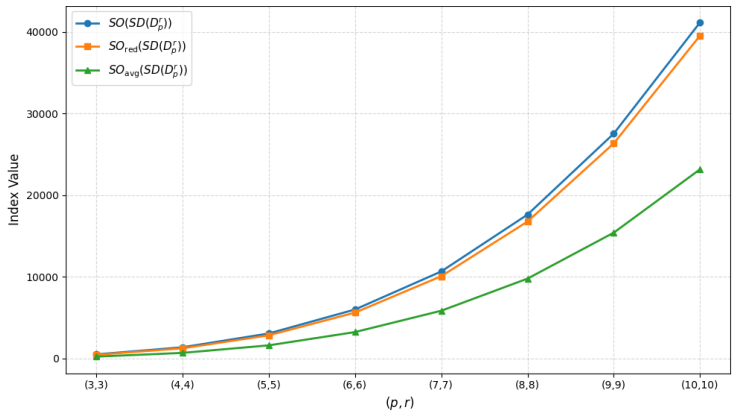


Figure 11. Comparison of Sombor indices for $SD(D_p^r)$

Note: SO = Sombor index; SO_{red} = reduced Sombor index; SO_{avg} = average Sombor index. $(SD(D_p^r))$ represents Sombor indices of the strong double graph of Dutch windmill graph.

3 Conclusions

In this study, we investigated the Sombor index (SO), reduced Sombor index (SO_{red}), and average Sombor index (SO_{avg}) for several special graph families, including web graphs, windmill graphs, Dutch windmill graphs, and the double and strong double graphs of Dutch windmill graphs. The key mathematical observation is that the values of these degree-based indices are strongly influenced by the degree distribution of the underlying graph. Since the Sombor type indices are defined in terms of the degrees of adjacent vertices, changes in vertex degrees and in the connectivity between vertices directly affect their numerical values.

For all the considered graph families and parameter ranges, the numerical results consistently show the ordering

$$SO(G) > SO_{\text{red}}(G) > SO_{\text{avg}}(G)$$

Furthermore, the values of all three indices increased as the parameters of the corresponding graph families enlarged, hence reflecting the effect of the growing graph structure and its degree distribution. The double graph construction introduces additional connections between the two copies of the Dutch windmill graph and consequently produces substantially larger values of the Sombor indices. The strong double construction provides an even stronger coupling between the two copies through the adjacency relations, resulting in a further increase in the index values. Thus, the numerical comparisons demonstrate that increasing connectivity through double and strong double graph operations has a significant effect on degree-based Sombor indices.

Overall, the obtained formulas and numerical comparisons indicated that the Sombor indices provided a useful means of distinguishing the structural changes caused by different graph constructions. In particular, the changes in degree distribution and connectivity induced by the double and strong double operations are explicitly mirrored in the magnitudes and growth patterns of SO, SO_{red}, and SO_{avg}.

Author Contributions

Conceptualization, K.N. and H.M.B.; methodology, K.N. and H.M.B.; software, H.M.B. and S.A.; validation, K.N., H.M.B., and S.A.; formal analysis, K.N. and H.M.B.; investigation, K.N., H.M.B., and S.A.; resources, K.N., H.M.B., and S.A.; data curation, K.N. and S.A.; writing—original draft preparation, K.N. and H.M.B.; writing—review and editing, K.N. and H.M.B.; visualization, S.A. and K.N.; supervision, K.N.; project administration, H.M.B. and S.A. All authors have read and agreed to the published version of the manuscript.

Data Availability

The data used to support the findings of this study are available from the corresponding author upon request.

Conflicts of Interest

The authors declare no conflicts of interest.

References

[1] J. H. Barnett, "Early writings on graph theory: Euler circuits and the Königsberg bridge problem," in *Resources for Teaching Discrete Mathematics*. Mathematical Association of America, 2009, pp. 197–208. https://doi.org/10.5948/UPO9780883859742.026

[2] A. Chen and F. Zhang, "Wiener index and perfect matchings in random phenylene chains," *MATCH Commun. Math. Comput. Chem.*, vol. 61, pp. 623–630, 2009.

[3] H. Bian and F. Zhang, "Tree-like polyphenyl systems with extremal Wiener indices," *MATCH Commun. Math. Comput. Chem.*, vol. 61, pp. 631–642, 2009.

[4] H. Deng, "Wiener indices of spiro and polyphenyl hexagonal chains," *Math. Comput. Model.*, vol. 55, no. 3–4, pp. 634–644, 2012. https://doi.org/10.1016/j.mcm.2011.08.037

[5] F. R. Burden, "A chemically intuitive molecular index based on the eigenvalues of a modified adjacency matrix," *Quant. Struct.-Act. Relatsh.*, vol. 16, no. 4, pp. 309–314, 1997. https://doi.org/10.1002/qsar.19970160406

[6] M. Saqlain, V. Simic, and D. Pamucar, "Evaluation of carbon footprints associated with cryptocurrency mining using q-rung orthopair fuzzy hypersoft sets," *Spectr. Eng. Manag. Sci.*, vol. 2, no. 1, pp. 122–134, 2024. https://doi.org/10.31181/sems21202410h

[7] M. Abid and M. Saqlain, "Optimizing diabetes data insights through kmapper-based topological networks: A decision analytics approach for predictive and prescriptive modeling," *Manag. Sci. Adv.*, vol. 1, no. 1, pp. 1–19, 2024. https://doi.org/10.31181/msa1120241

[8] M. Saeed, M. R. Ahmad, M. Saqlain, and M. Riaz, "Rudiments of N-framed soft sets," *Punjab Univ. J. Math.*, vol. 52, no. 5, pp. 15–30, 2020.

[9] Z. Raza, "The harmonic and second Zagreb indices in random polyphenyl and spiro chains," *Polycycl. Aromat. Compd.*, vol. 42, no. 3, pp. 671–680, 2022. https://doi.org/10.1080/10406638.2020.1749089

[10] M. Javaid and U. Ali, "The first general Zagreb connection index and its particular cases on some special graphs," *Comput. J. Comb. Math.*, vol. 1, pp. 1–10, 2021.

[11] S. Fajtlowicz, "On conjectures of graffiti," *Ann. Discrete Math.*, vol. 38, pp. 113–118, 1988. https://doi.org/10.1016/S0167-5060(08)70776-3

[12] J. Sedlar, D. Stevanović, and A. Vasilyev, "On the inverse sum indeg index," *Discrete Appl. Math.*, vol. 184, pp. 202–212, 2015. https://doi.org/10.1016/j.dam.2014.11.013

[13] C. K. Gupta, V. Lokesha, S. B. Shwetha, and P. S. Ranjini, "On the symmetric division deg index of graph," *Southeast Asian Bull. Math.*, vol. 40, no. 1, p. 59, 2016.

[14] D. Vukičević and B. Furtula, "Topological index based on the ratios of geometrical and arithmetical means of end-vertex degrees of edges," *J. Math. Chem.*, vol. 46, pp. 1369–1376, 2009. https://doi.org/10.1007/s10910-009-9520-x

[15] J. Rada, J. M. Rodríguez, and J. M. Sigarreta, "Sombor index and elliptic Sombor index of benzenoid systems," *Appl. Math. Comput.*, vol. 475, p. 128756, 2024. https://doi.org/10.1016/j.amc.2024.128756

[16] J. Rada, J. M. Rodríguez, and J. M. Sigarreta, "On integral Sombor indices," *Appl. Math. Comput.*, vol. 452, p. 128036, 2023. https://doi.org/10.1016/j.amc.2023.128036

[17] I. Milovanovic, E. Milovanovic, and M. Matejic, "On some mathematical properties of Sombor indices," *Bull. Int. Math. Virtual Inst.*, vol. 11, no. 2, pp. 341–353, 2021. https://doi.org/10.7251/BIMVI2102341M

[18] K. C. Das, A. S. Çevik, I. N. Cangul, and Y. Shang, "On Sombor index," *Symmetry*, vol. 13, no. 1, p. 140, 2021. https://doi.org/10.3390/sym13010140

[19] J. Rada, J. M. Rodríguez, and J. M. Sigarreta, "General properties on Sombor indices," *Discrete Appl. Math.*, vol. 299, pp. 87–97, 2021. https://doi.org/10.1016/j.dam.2021.04.014

[20] M. A. Ali, M. S. Sardar, I. Siddique, and D. Alrowaili, "Vertex-based topological indices of double and strong double graph of Dutch windmill graph," *J. Chem.*, vol. 2021, no. 1, p. 7057412, 2021. https://doi.org/10.1155/2021/7057412

[21] I. Redžepović, "Chemical applicability of Sombor indices," *J. Serb. Chem. Soc.*, vol. 86, no. 5, pp. 445–457, 2021. https://doi.org/10.2298/JSC201215006R

[22] Z. Wang, Y. Mao, Y. Li, and B. Furtula, "On relations between Sombor and other degree-based indices," *J. Appl. Math. Comput.*, vol. 68, pp. 1–17, 2022. https://doi.org/10.1007/s12190-021-01516-x

[23] I. Gutman, I. Redžepović, G. Ö. Kizilirmak, and V. R. Kulli, "Euler-Sombor index and its congeners," *Open J. Math. Sci.*, vol. 9, pp. 141–148, 2025. https://doi.org/10.30538/oms2025.0249

[24] V. S. Shigehalli and S. A. Chougale, "Sombor index and its applications," *Open J. Discrete Appl. Math.*, vol. 8, pp. 50–63, 2025. https://doi.org/10.30538/psrp-odam2025.0111